Aerosol and Air Quality Research, 10: 245–254, 2010
Copyright © Taiwan Association for Aerosol Research
ISSN: 1680-8584 print / 2071-1409 online
doi: 10.4209/aaqr.2009.10.0065

Analysis of Relationship between Inorganic Gases and Fine Particles in Cleanroom Environment

I-Kai Lin, Hsunling Bai*, Bi-Jun Wu

Institute of Environmental Engineering, National Chiao Tung University, 1001 University Rd., Hsinchu 300, Taiwan

ABSTRACT

The concentrations and characteristics of major components in inorganic gases and fine particles were measured at the photo and etch cleanroom areas in a Taiwan semiconductor factory. The results showed that the major inorganic gases, as expressed in terms of volume concentration, were NH_3 and HF at 7–10 and 4–6 ppbv, respectively. The average $PM_{2.5}$ mass concentration were 17.52 and 18.23 μg/m^3 at the photo and etch areas, respectively, with species of Na^+, NH_4^+, Cl^- and SO_4^{2-} had the highest concentrations in the $PM_{2.5}$ mass. And the inorganic species account for 56% and 62% of the particulate mass, respectively, at the photo and etch areas. Relatively stronger correlations were observed between NH_4^+ and SO_4^{2-} with the correlation coefficient R^2 of 0.62 and 0.82, respectively, at the photo and etch areas; this indicates their common source was possibly from the gas to particle formation process. And NH_3 was found to co-exist with HF at the etch area due to their common source as process chemicals (NH_4OH and HF) in the wet bench. In the predominant NH_3-rich environment, ammonia is the basic neutralizing agent to form the ammonium aerosol in a cleanroom.

Keywords: Diffusion denuder system (DDS); AMCs (Airborne Molecular Contaminants); Micro-contamination; Cleanroom; Semiconductor device.

INTRODUCTION

The cleanness of a cleanroom environment must be tightly controlled to achieve high-yield and high-performance ULSI (Ultra large scale integrated circuit) manufacturing (Kinkead *et al.*, 1995; Kitajima and Shiramizu, 1997; Yeh *et al.*, 2004; Chien *et al.*, 2007). Airborne molecular contaminants (AMCs) can impact almost all aspects of sub-micron device fabrication from fab operation to final device performance.

There are many sources of AMCs such as chemicals commonly used in semiconductor process including cleaning process (H_2SO_4, HCl, NH_4OH, HNO_3, HF, IPA, methanol and acetone, etc.), photolithography process (Solvent, KOH and NaOH, etc.), etching process (H_2SO_4, HNO_3, HCl, HF, Cl_2, HBr, CF_4, SF_6, F_2, BCl_3, etc.), deposition process (SiH_4, NH_3, WF_6, B_2H_6, etc.) and ion implantation and diffusion process (AsH_3, PH_3, BF_3, etc.). The major air pollutants emitted from integrated circuit industries include the VOCs (Volatile Organic Compounds), such as isopropyl alcohol (IPA), acetone, propylene glycol methyl ether acetate (PGMEA), ethyl acetate and the inorganic acids such as hydrofluoric acid (HF), sulfuric acid (H_2SO_4) and hydrochloric acid (HCl). The technical operators deliver FOUP (Front Open Unified Pod) to a specific tool for processing or measurement and other engineers manage equipment and process production. To prevent wafer contamination by outside dust from clean room workers, they have to put on special dust-free clothing. However it is still possible to induce contamination from the workers themselves and from their inappropriate process handling.

It is evident that the ionic contaminants such as Na^+ and K^+ could deposit on wafers within the device-fabrication region and cause copper corrosion and metal cross contamination. The deposition rates of ionic contaminants on silicon wafer and their adsorption/desorption behaviors on the silicon wafer were reported in our prior study (Lin *et al.*, 2009). Inorganic gases could lead to harmful precipitates and result in irreversible damage to process wafers (MacDonald *et al.*, 1993; Saiki *et al.*, 1995). In addition, the major acidic gases in the cleanroom air such as HF, HCl, HNO_2, HNO_3 and SO_2 could be neutralized by the principal alkaline species of NH_3. Through gas-to-particle conversion process, the acidic gases and NH_3 may involve in the formation of fine particles.

The condensation-induced particle formation during vacuum pump down containing aggressive compounds from humid air and inorganic pollutants has been investigated (Ye *et al.*, 1993). Fine particles are also

* Corresponding author. Tel: +886-3-5731868;
Fax: +886-3-5725958
E-mail address: hlbai@mail.nctu.edu.tw

generated by gas phase nucleation in thin film preparation processes (Adachi *et al.*, 1994). Gas-to-particle conversion can be accomplished by condensation which adds mass onto pre-existing aerosols, or by direct nucleation from gaseous precursors to form an aerosol. Gas-to-particle conversion strongly depends on the concentration of acidic/basic gases and water vapors in the atmosphere (Seinfeld and Pandis, 2006). To better understand such processes, accurate methods in analyzing cleanroom aerosol composition are essential. The diffusion denuder system (DDS) is a suitable method for the determination of gaseous NH_3, HF, HCl, HNO_2, HNO_3, SO_2 and $PM_{2.5}$ particulates in the cleanroom environment with negligible mutual interferences (Lin *et al.*, 2008).

Although the inorganic gaseous concentrations in the cleanroom have been investigated (Lue *et al.*, 1998; Lue and Huang, 1999; Lin *et al.*, 2008), their focuses were either on the accuracy of sampling and analysis method or on gaseous compounds in the clean room only. However, the wafer could be contaminated both by the accumulation of gaseous contaminants and by the direct deposition of particulates in the clean room air. And the relationship between the inorganic gases and chemical species in particulate in a cleanroom environment has not been examined. Besides, the particulates in the clean room could be from either primary aerosol or gas-to-particle formation mechanism. In this study, the concentrations of acidic gases, basic gases and aerosol species are measured by DDS in a typical class 100 cleanroom. The measured data are used to examine the possible sources and the inter-correlations of AMCs.

EXPERIMENTAL METHODS

Sampling and Analysis

The study area consisted of two measurement sites, a cleanroom photo area and an etch area of class 100, in a Taiwan semiconductor fab. The sampling locations of the photo and etch areas are near the Scanner PAS5500/500D DUV (Deep Ultra Violet) tool (ASML Corporation) and the wet bench tool, respectively. The data measured in these two sampling sites could reveal the different chemical compositions of AMCs induced from different sources. The relative humidity in the sampling areas was 45 ± 3% and temperature was 22 ± 1°C. An average value of laminar flow velocities was 0.45 m/s with less than 10% variations.

Samples were collected using the commercial diffusion denuder system (DDS, MSP corporation, USA). The DDS is consisted of three major parts: an impactor, four denuder plates and a filter pack. The impactor removes coarse particles larger than 2.5 μm aerodynamic diameter. The 1st and 2nd denuder plates were coated with 0.1% (w/v) NaCl in 1:9 methanol/water for collecting HNO_3 and SO_2 gases. The 3rd plate was coated with 1% (w/v) Na_2CO_3/1% (w/v) glycerol in a 50% water/50% methanol mixture for collecting HF, HCl, HNO_2 and SO_2 gases. The 4th plate was coated with 1% (w/v) citric acid in methanol solution for collecting NH_3 (Lin *et al.*, 2008). The concentrations of all species measured from the DDS sampler were obtained based on the sum of all collected plates. The filter pack contains a Teflon (Gelman Science, 2 μm pore size) and a Nylon filter (Gelman Science, 1 μm pore size) in series. The Teflon filter was used for collecting fine particles of less than 2.5 μm ($PM_{2.5}$) in a cleanroom. The Nylon filter next to the Teflon filter was installed to capture gaseous species which dissociated from the particles collected on the Teflon filter. Before and after field sampling, the filters were weighed on an electronic balance (Mettler Toledo AE240) with a reading precision of 10 μg to determine the mass concentration after having been conditioned at 22°C and 45% relative humidity for 24 hours.

The samplers were operated at a constant flow rate of 10 L/min and 24 hours sampling time to determine possible components of the hazing contaminants onto the wafer surface (Lin *et al.*, 2009). A total of 10 samples was used for the average species concentrations at the photo and etch areas, respectively, in this study. Detailed QA/QC description of the sampling collection efficiency, extraction procedures and ion chromatography analysis can be referred to our prior study (Lin *et al.*, 2008). In addition, the particle concentrations in the cleanroom were also analyzed by the particle measuring systems (PMS, Micro laser Particle Counter Turbo 110, USA).

Equilibrium Chemistry

Gas-to-particle conversion may result from homogeneous gas-phase processes, or it may be controlled by processes in the particulate phase. Gas-phase processes, either physical or chemical, can produce a supersaturated state which was then collapsed by aerosol formation (Friedlander, 2000). For example, when gaseous NH_3 and H_2SO_4 are mixed, white crystallite materials are formed. The equilibrium relationship is given by

$$(NH_4)_2SO_{4(s)} \leftrightarrows 2NH_{3(g)} + H_2SO_{4(g)} \quad (1)$$

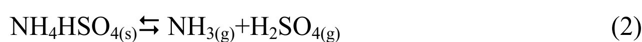

$$NH_4HSO_{4(s)} \leftrightarrows NH_{3(g)} + H_2SO_{4(g)} \quad (2)$$

Assuming that the two reaction products form an ideal component, the equilibrium constants (K_p) of reaction equations (1) and (2) can be written as

$$K_{p1} = P_{e,NH_3}^{\ 2} P_{e,H_2SO_4} \quad (3)$$

$$K_{p2} = P_{e,NH_3} P_{e,H_2SO_4} \quad (4)$$

where $P_{e,i}$ refers to the equilibrium vapor pressure of each gas species *i*. The ratio of the actual pressure of the vapor, P_i, is correlated to the equilibrium vapor pressure at the same temperature by the saturation ratio (*S*). The saturation ratio of $(NH_4)_2SO_4$ and NH_4HSO_4 can be written as

$$S_{(NH_4)_2SO_4} = P_{NH_3}^{\ 2} P_{H_2SO_4} / K_{p1} \quad (5)$$

$$S_{NH_4HSO_4} = P_{NH_3} P_{H_2SO_4} / K_{p2} \quad (6)$$

When the saturation ratio is greater than unity ($S > 1$), the system is said to be supersaturated and aerosol could be formed by the reaction between acidic and basic gases (Friedlander, 2000).

RESULTS AND DISCUSSION

Inorganic Gaseous Species Concentrations

During the study, an NH_3 real time monitor (IMS, Ion Mobility Spectrometer, Model 55 series, Molecular Analytics, USA) was also employed. The real time monitoring instrument of IMS took data for every 60 seconds, and the measured data of NH_3 gas were 24 hours averaged in order to compare with those of the DDS, the comparison results are shown in Fig. 1. One can see that these two NH_3 measurement data are in good agreement with R^2 of 0.98. One-way ANOVA showed no significant differences ($P > 0.05$). Although the real time monitor is convenient, it can only measure the NH_3 gas concentration. And thus the DDS is employed in the following study to sample all gaseous and particulate species of inorganic AMCs.

The sampling time of 24 hours for the DDS is required because the chemical compositions of the wafer contaminants can be analyzed only after long time exposure (Lin *et al.*, 2009). However, sampling bias due to the reaction of residual NH_3 with the acidic particulate species in the downstream filter pack is possible during long sampling time. In this study, the denuder sampling efficiency for NH_3 was well over 90% at all time (Lin *et al.*, 2008), leaving minor amounts of NH_3 to the downstream filter packs. Thus the possibility of artifact due to residual NH_3 has been kept at minimal.

Fig. 2 shows the average concentrations of gaseous NH_3, HF, HCl, HNO_2, HNO_3 and SO_2. At the photo area, the average concentrations of NH_3, HF, HCl, HNO_2, HNO_3 and SO_2 in the whole sampling period were 7.98, 4.97, 1.57, 1.41 and 0.35 ppb, respectively. The gaseous concentration of NH_3 was the highest, which can be attributed to HMDS (Hexamethyldisilazane, $(CH_3)_3SiNHSi(CH_3)_3$) and TMAH (Tetramethylammonium hydroxide) usage during DUV tool process and human emissions from exhaled breath. And since no process chemical of HF is used in the photo area, the HF gas could be mainly from outdoor contaminants in the stack exhaust gas of semiconductor or optoelectronic industries (Huang *et al.*, 2005).

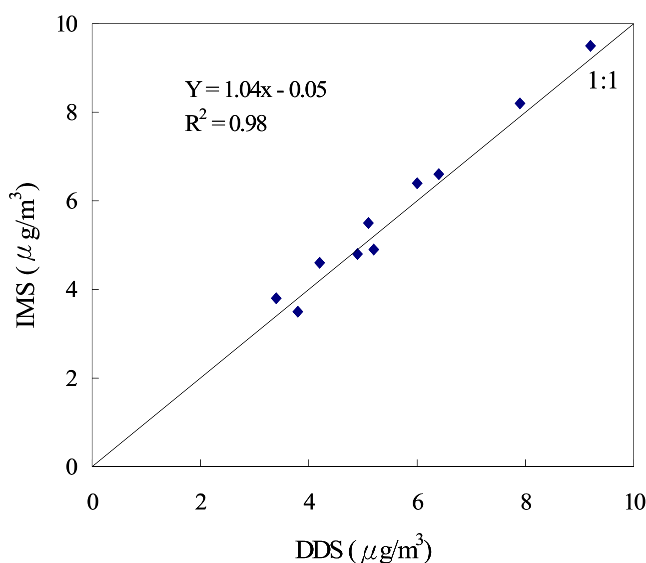

Fig. 1. Comparison of NH_3 measured data between the IMS real time monitor and the DDS system.

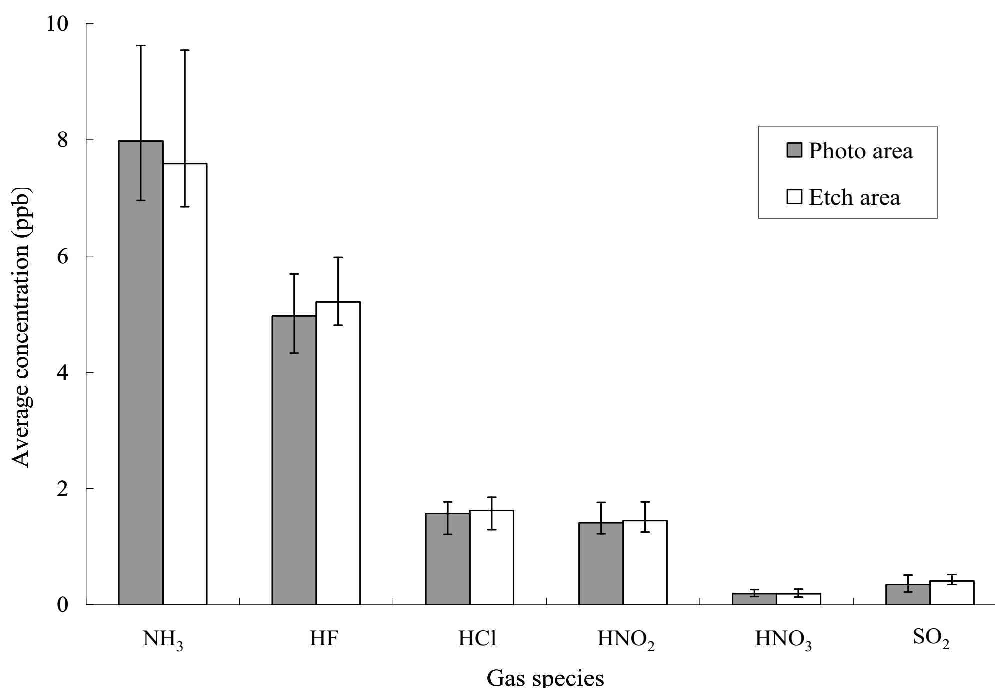

Fig. 2. Comparison of gas concentrations at the photo and etch areas.

At the etch area, the average concentrations of gaseous NH_3, HF, HCl, HNO_2, HNO_3 and SO_2 in the sampling period were 7.59, 5.21, 1.62, 1.45, 0.19 and 0.41 ppb, respectively. The gaseous concentrations of NH_3 and HF were higher than the others, which could be attributed to SC1 (Standard Clean 1, $NH_4OH:H_2O_2:H_2O$) cleans and HF usage in the wet bench and human exhaled emissions of NH_3 as well. The wet chemical station tended to have higher levels of NH_3 and HF contaminants which are probably due to the vaporized acids or bases used in wafer cleaning and rinsing. The outdoor environment could also be the sources of NH_3 as it had been detected to be the inorganic gas with the highest concentration (Tsai *et al.*, 2003).

Particulate Mass and Ionic Species Concentrations

For the sampling of fine particles, the average $PM_{2.5}$ mass at the photo and etch areas were 17.52 ± 2.38 and 18.23 ± 2.80 μg/m^3, respectively as shown in Table 1. The species of Cl^- and NO_3^- were observed on Nylon filters which are due to the high volatility of them. From the sum of particle masses collected on the Teflon and Nylon filters of the DDS, the average concentrations of F^-, Cl^-, NO_3^-, SO_4^{2-}, Na^+, NH_4^+, K^+ and Ca^{2+} at the photo area were found to be 0.23, 2.59, 0.41, 0.92, 2.45, 2.17, 0.61 and 0.45 μg/m^3, respectively. This implies that the major acidic species at the photo area were Cl^- and SO_4^{2-} and the major basic species were Na^+ and NH_4^+ ions.

The major ionic species at the etch area, Na^+, NH_4^+, Cl^- and SO_4^{2-}, were the same as those at the photo area. The NH_4^+ and Na^+ were emitted from human exhaled emissions and transferred by sweat, tears (ionic form) and skin peeling (Constant *et al.*, 2000) could be the major source of them. On the other hand, the acidic ion concentrations seem to be higher in the etch area. This may be due to major acidic species containing SC2 (Standard Clean 2, $HCl:H_2O_2:H_2O$) clean process chemicals or etching acids (H_2SO_4 and HNO_3) were widely used at the etch area.

No clear correlations of particle number concentrations were observed between sampling locations of photo and etch areas. The particle number concentrations showed that average concentrations of <0.1 μm, 0.1–0.2 μm, 0.2–0.3 μm, 0.3–0.5 μm, 0.5–1 μm and 1–2 μm in the clean room were 4540, 2920, 1617, 560, 175 and 35 particles/m^3, respectively. It was shown from the aerosol particle size distribution that the particle number concentration was increased as particle diameter was smaller. The presence of small particles revealed the high probability of nucleation from gaseous contamination species. The particles can also be induced by a moving operator, which cause the slight variation in the particle number concentrations (Fu *et al.*, 2001). It is also noted that the $PM_{2.5}$ mass does not seem to correlate to the particle number concentrations measured by the laser particle counter. The total $PM_{2.5}$ mass measured by the DDS was much larger than those estimated by the laser particle counter. The reason for this is still not well understood.

The other unknown compositions accounted for 43.9% at the photo area, and 37.6% at the etch area as shown in Table 1. The unknown composition possibly includes EC (elemental carbon), OC (organic carbon), carbonate and moisture. A wide range of volatile organic vapors has also been detected in process areas such as lithography and wet stations. The co-existence of organic and inorganic elements enlarges the wafer contaminants up to 30–50 μm. The particle sizes were not directly proportional to the period of exposure of the wafer (Bai *et al.*, 2002).

It is worth noting that due to the organic base compounds

Table 1. Average mass concentrations of particulate species at the photo and etch areas (N =10 samples).

Species		Photo area (Mean ± SD[a])		Etch area (Mean ± SD)	
		Teflon filter (μg/m^3) (%)	Nylon filter (μg/m^3) (%)	Teflon filter (μg/m^3) (%)	Nylon filter (μg/m^3) (%)
Anions	F^-	0.23 ± 0.10 (1.3%)	–	0.28 ± 0.11 (1.5%)	–
	Cl^-	2.11 ± 0.51 (12.0%)	0.48 ± 0.16 (2.7%)	2.15 ± 0.34 (11.8%)	0.47 ± 0.08 (2.6%)
	NO_2^-	–	–	–	–
	NO_3^-	0.41 ± 0.14 (2.3%)	–	0.95 ± 0.18 (5.2%)	0.22 ± 0.07 (1.2%)
	SO_4^{2-}	0.92 ± 0.32 (5.3%)	–	1.67 ± 0.35 (9.2%)	–
	Total of acidic species	4.15 ± 0.78 (23.6%)		5.74 ± 0.81 (31.5%)	
Cations	Na^+	2.45 ± 0.51 (14.0%)	–	2.30 ± 0.51 (12.6%)	–
	NH_4^+	2.17 ± 0.35 (12.4%)	–	1.95 ± 0.41 (10.7%)	–
	K^+	0.61 ± 0.14 (3.5%)	–	0.70 ± 0.23 (3.9%)	–
	Mg^{2+}	–	–	–	–
	Ca^{2+}	0.45 ± 0.13 (2.6%)	–	0.68 ± 0.17 (3.7%)	–
	Total of basic species	5.68 ± 0.55 (32.5%)		5.63 ± 0.73 (30.9%)	
Other compositions		7.69 ± 1.87 (43.9%)		6.83 ± 1.97 (37.6%)	
$PM_{2.5}$ Mass (Mean ± SD)		17.52 ± 2.38		18.23 ± 2.80	

[a] Standard deviation

such as NMP (N-methyl-2-pyrrolidinone), PGME (Propylene glycol methyl ether), PGMEA, PR (Photo resist) and ammines were widely used for resist coating and stripping, the OC percentage of the unknown composition at the photo area may be higher than those at the etch area.

Correlation between Inorganic Gases and Particulate Species

Table 2 displays the correlation coefficients (R^2) between chemical species of gases and fine particles at the photo and etch areas. At the photo and etch areas, the concentration of NH_4^+ has high correlation coefficient values of 0.62 and 0.82 with SO_4^{2-}, respectively, which means NH_4^+ concentration is highly related to SO_4^{2-}. The correlations of NH_4^+ with SO_4^{2-} at the etch area were larger than those at the photo area. And they are suspected to be from the gas-to-particle formation between the reaction of NH_3 and H_2SO_4. This seems to imply that reactions of additional local emissions might be possible to produce ammonium sulfate aerosols.

There are strong negative correlations between HNO_3 and NH_4^+ as well as between NH_3 and NO_3^- with their respective correlation coefficients of –0.73 and –0.68 at photo area. This indicated the possibility of condensation induced particle growth of either HNO_3 condensed onto NH_4^+ containing particles or NH_3 condensed onto NO_3^- containing particles. Thus the gaseous NH_3 or HNO_3 concentrations would be lower if the particulate phase concentrations of NO_3^- or NH_4^+ are higher. In addition, a relatively higher correlation between NH_3 and HF with R^2 of 0.70 at the etch area indicates a common and major source from the wet bench process chemicals (NH_4OH, HF and BOE). The presence of workers may also contribute to the concentration of NH_3, but its contribution seems not to be as strong as the process chemicals.

The calculations of NH_4Cl and NH_4NO_3 equilibrium constants were obtained from the equilibrium expressions provided by Pio and Harrison (1987) and Stelson and Seinfeld (1982), respectively. And the equilibrium constants of $(NH_4)_2SO_4$ and NH_4HSO_4 were calculated by the following formula (Poling *et al.* 2001):

$$\ln K_p = \frac{-\Delta G°(T)}{RT} \quad (7)$$

where $\Delta G°(T)$ is the Gibbs energy change of reaction, R is the universal gas constant and T is the absolute temperature. The calculations of equilibrium constants were tabulated in Table 3. And values of them at clean room temperature of 22°C (295K) together with the corresponding saturation ratios (S) using measured average gas concentrations are also listed in Table 3.

It would usually require saturation ratios of 2–10 to have homogeneous nucleation occurs, while heterogeneous nucleation can occur at super-saturations of only a few percents (Hinds, 1999). As can be seen in Table 3, at the photo and etch sampling areas, the average saturation ratios of NH_4NO_3 were 0.12 and 0.11, respectively. Thus NH_4NO_3

Table 2. Coefficients of correlation (R^2) for gas and particle concentrations.

		F^-	Cl^-	NO_3^-	SO_4^{2-}	Na^+	NH_4^+	HF	HCl	HNO_2	HNO_3	SO_2
Particle phase	Cl^-	–0.01[a]										
		0.08[b]										
	NO_3^-	–0.08	0.04									
		–0.007	0.33									
	SO_4^{2-}	–0.14	0.39	0.37								
		0.03	0.48	0.34								
	Na^+	0.02	–0.06	0.04	–0.20							
		–0.02	0.12	–0.003	0.001							
	NH_4^+	–0.02	0.49	0.37	**0.62**	–0.20						
		0.03	**0.61**	0.41	**0.82**	0.01						
Gas phase	HF	–0.001	0.23	0.06	0.02	0.18	0.03					
		–0.001	0.0003	–0.11	–0.30	0.03	–0.33					
	HCl	0.05	–0.47	–0.006	–0.30	0.18	–0.37	0.004				
		0.001	–0.29	–0.08	–0.08	–0.46	–0.20	0.02				
	HNO_2	–0.04	0.01	**0.60**	0.08	0.08	0.13	0.04	–0.001			
		–0.21	0.02	–0.02	0.006	0.23	–0.006	0.15	0.0001			
	HNO_3	0.003	–0.11	–0.35	–0.46	0.22	**–0.73**	0.02	0.09	–0.04		
		0.03	–0.05	–0.39	–0.20	0.14	–0.27	0.20	0.05	0.27		
	SO_2	–0.05	**–0.54**	–0.05	–0.42	0.13	**–0.56**	–0.08	0.41	0.003	0.31	
		–0.16	–0.10	–0.02	–0.44	0.07	–0.18	0.10	–0.08	–0.06	–0.02	
	NH_3	0.03	–0.06	**–0.68**	–0.47	0.02	–0.47	0.02	0.13	–0.48	0.47	0.16
		–0.10	–0.001	–0.02	–0.35	0.016	–0.32	**0.70**	–0.02	0.003	0.02	0.34

[a] Photo area of cleanroom
[b] Etch area of cleanroom

Table 3. Equilibrium constant of ammonium particles.

Reaction equation	Equilibrium constant (unit of T_0 ^0K)	K_p (ppb$^{2\ or\ 3}$)	S^a (Mean ± SD)
$NH_4Cl_{(s)} \leftrightarrows NH_{3(g)} + HCl_{(g)}$	$\ln K_p = 2.2358\ln T - 2.13204 \times 10^4 T^{-1} + 65.4375 - 9.167 \times 10^{-3} T + 4.644 \times 10^{-7} T^2 - 1.105 \times 10^{-10} T^3$ (Pio and Harrison, 1987)	3.21	3.92 ± 0.73^b 3.83 ± 0.60^c
$NH_4NO_{3(s)} \leftrightarrows NH_{3(g)} + HNO_{3(g)}$	$\ln K_p = 84.6 - (24220/T) - 6.1\ln(T/298)$ (Stelson and Seinfeld, 1982)	12.93	0.12 ± 0.03 0.11 ± 0.03
$(NH_4)_2SO_{4(s)} \leftrightarrows 2NH_{3(g)} + H_2SO_{4(g)}$	$\ln K_p = 55.7 - 42526/T$	3.83×10^{-39}	-[d]
$NH_4HSO_{4(s)} \leftrightarrows NH_{3(g)} + H_2SO_{4(g)}$	$\log K_p = 17.761 - 12326/T$	3.69×10^{-11}	-[d]

[a] The saturation ratio (*S*) was expressed as the average values ± SD (standard deviation).
[b] Photo area of cleanroom
[c] Etch area of cleanroom
[d] For the reactions between NH_3 and H_2SO_4, values of *S* could not be estimated because the concentration of H_2SO_4 could not be measured and separated from the other SO_4^{2-} compounds.

particles were not favored to be formed in the clean room. The NH_4^+ and NO_3^- measured in the particulate phase should not be highly correlated with each other. And this can be observed from the regression coefficients of NH_4^+ and NO_3^- at the photo and etch areas to be only 0.37 and 0.41, respectively as shown in Table 2.

On the other hand, the average saturation ratios of NH_4Cl were 3.92 and 3.83 at the photo and etch areas, respectively, thus there is a relatively higher possibility for the formation of NH_4Cl particles as compared to the formation of NH_4NO_3 particles. But the possibility of homogeneous nucleation of NH_4Cl would be much less than the heterogenous nucleation or the condensation of NH_4Cl monomers onto existing nuclei or particle surfaces. The regression coefficients of NH_4^+ and Cl^- concentrations, 0.49 and 0.61, respectively, at the photo and etch areas as shown in Table 2 are therefore relatively higher than those of NH_4^+ and NO_3^-.

Because the H_2SO_4 concentration could not be measured directly, the values of saturation ratios for the NH_3 and H_2SO_4 equilibrium system cannot be calculated and listed in Table 3 as for the ammonium nitrate and ammonium chloride species. However, ammonium sulfate and bisulfate should be the most stable inorganic salts due to their very low values of K_p at 3.83×10^{-39} and 3.69×10^{-11}, respectively. Thus there is a very high possibility for the formation of $(NH_4)_2SO_4$ and NH_4HSO_4 monomers from gas phase reaction, and the monomers then form stable $(NH_4)_2SO_4$ and NH_4HSO_4 particles by the homogeneous nucleation mechanism. This can also be observed from the high correlations between NH_4^+ and SO_4^{2-} concentrations in Table 2. The results were very similar to those found by Johnstone *et al.* (2004) in a semiconductor manufacturing plant which indicated that the optical lens hazing might be due to the fine salt particles generated from the reaction of NH_3 and H_2SO_4.

The reaction products between NH_3 and H_2SO_4 could include $(NH_4)_2SO_4$ (molar NH_4^+/SO_4^{2-} ratio = 2), $(NH_4)_3H(SO_4)_2$ (molar NH_4^+/SO_4^{2-} ratio = 1.5) and NH_4HSO_4 (molar NH_4^+/SO_4^{2-} ratio = 1) (Warneck, 2000). In this study, it was found that ammonium was co-existed with sulfate and the average molar ratio of NH_4^+/SO_4^{2-} were 6.60 and 3.13 at the photo and etch areas, respectively as shown in Table 4. This suggests that $(NH_4)_2SO_4$ is the preferred form of sulfate and the remaining NH_4^+ can react with HNO_3 and HCl (Li *et al.*, 2007).

If [TA] and [TS] are the total (gas + aqueous + solid) molar concentrations of ammonia and sulfate, respectively, then [TA] > 2[TS] suggests that this site is located in the predominant NH_3-rich environment (Seinfeld and Pandis, 2006). The average molar ratio of [TA]/[TS] are almost 25.12 and 13.83 at the photo and etch areas, respectively as shown in Table 4. The extremely high concentrations of NH_3 gas indicating the heteromolecular nucleation of ammonia gas with some acidic gases can form particles (Zhuang *et al.*, 1999).

Fig. 3(a) shows the charge balance between NH_4^+ and sum of F^-, Cl^-, NO_3^- and SO_4^{2-} anions. The slopes of the regressions were 0.78 with R^2 values of 0.64 and 0.74 at the photo and etch areas, respectively. It is interesting to observe that the slopes of NH_4^+ with the anions of F^-, Cl^-, NO_3^- and SO_4^{2-} are the same, which may indicate that they have the same sources of contamination from the outdoor environment. The high correlations of NH_4^+ species with the sum of F^-, Cl^-, NO_3^- and SO_4^{2-} anions in this two areas are mainly due to the high correlation of NH_4^+ species with the SO_4^{2-} anion as shown previously in Table 2. And although ammonium sulfates appear be the most significant ammonium salts, the charge balance result shown in Fig. 3(a) indicated that the ammonium salts could also be due to the condensation of NO_3^-, F^- and Cl^- acidic gases to neutralize the particles. The charge balance between NH_4^+ and the acidic species of F^-, Cl^-, NO_3^- and SO_4^{2-} is nearly 1:1 in the

Table 4. Molar ratios of cations and anions in fine particles at the photo and etch areas.

Solid particles	Molar ratios	Photo area (Mean ± SD[a])	Etch area (Mean ± SD)
Ammonium particles	$[NH_4^+]/2[SO_4^{2-}]$	6.60 ± 1.18	3.13 ± 0.32
	[TA] /[TS][b]	25.12 ± 6.10	13.83 ± 2.80

[a] Standard deviation
[b] [TA] and [TS] are the total (gas + aqueous + solid) molar concentrations of ammonia and sulfate, respectively.

photo area, but there is still an excess amount of acidic species presented in the etch area.

In order to complete the ion balance, all molar concentrations of cations (Na^+, NH_4^+, K^+ and Ca^{2+}) and anions (F^-, Cl^-, NO_3^- and SO_4^{2-}) are included into the charge balance of ions and the results are shown in Fig. 3(b). The slopes were 0.32 and 0.44 with R^2 values of 0.19 and 0.50 between sum of cations and sum of anions at the photo and etch areas, respectively. They were lower than those in Fig. 3(a) that contains only NH_4^+ as the cation. It is also noted that the charge balance shifted toward 2:1 relationship.Possible explanation is due to the presence of high Na^+ and K^+ molar fractions in the cations, they were from operators' sweat, tears (ionic form) and skin peeling. They also caused the low correlations between sum of cations and sum of anions.

Fig. 4 shows molar concentration fraction of the gas and particle of the same species to evaluate the distribution of gas and particulate phase of each species. The Cl^-, NO_3^- and sulfur species were over 40% fractional distribution in the particulate phase in both photo and etch areas. The aged air mass from the clean room, which would have high particle fractions, could have an impact at the photo and etch areas. And it was aware from Table 1 that Cl^- has the highest anion concentration in particulate phase. On the other hand, the HF and NH_3 in gas phase are in much

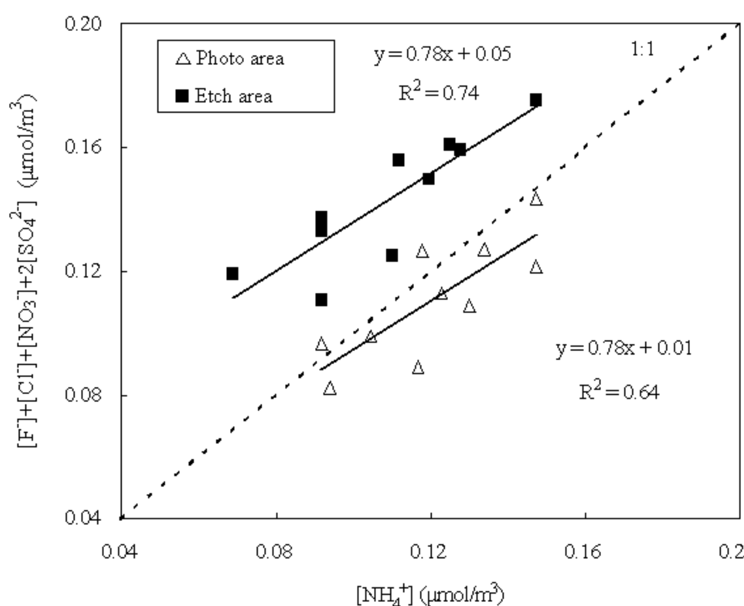

Fig. 3(a). Charge balance between NH_4^+ and sum of anions (F^-, Cl^-, NO_3^- and SO_4^{2-}) at the photo and etch areas.

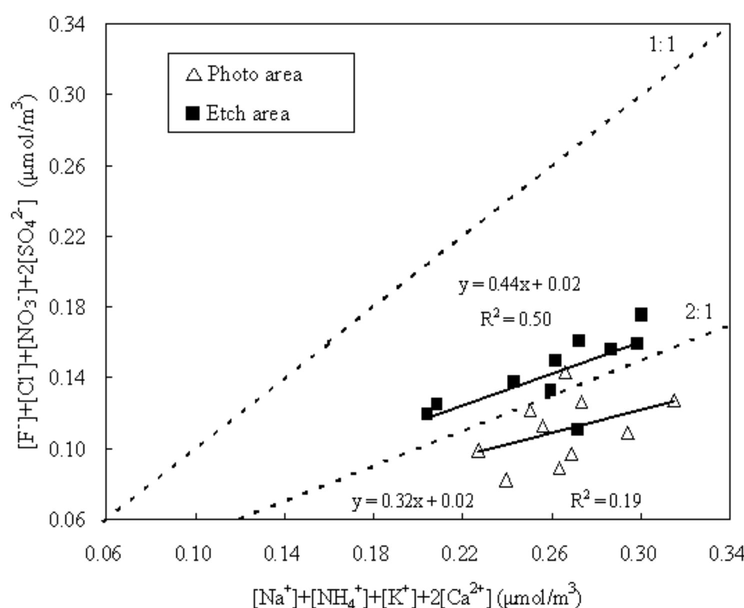

Fig. 3(b). Charge balance between sum of cations (Na^+, NH_4^+, K^+ and Ca^{2+}) and sum of anions (F^-, Cl^-, NO_3^- and SO_4^{2-}) at the photo and etch areas.

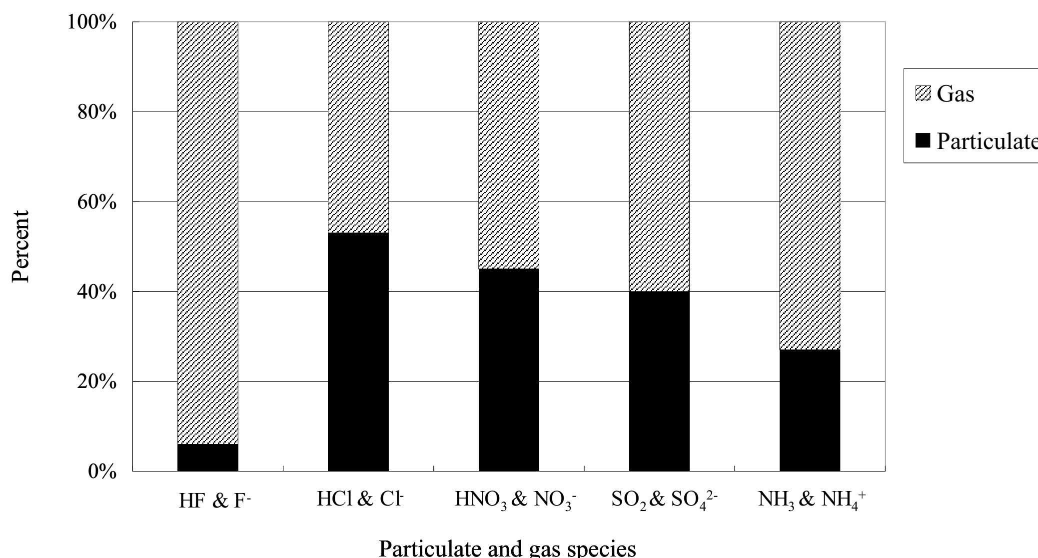

Fig. 4(a). Fractional distribution of each inorganic species in gas and particulate phases at photo area.

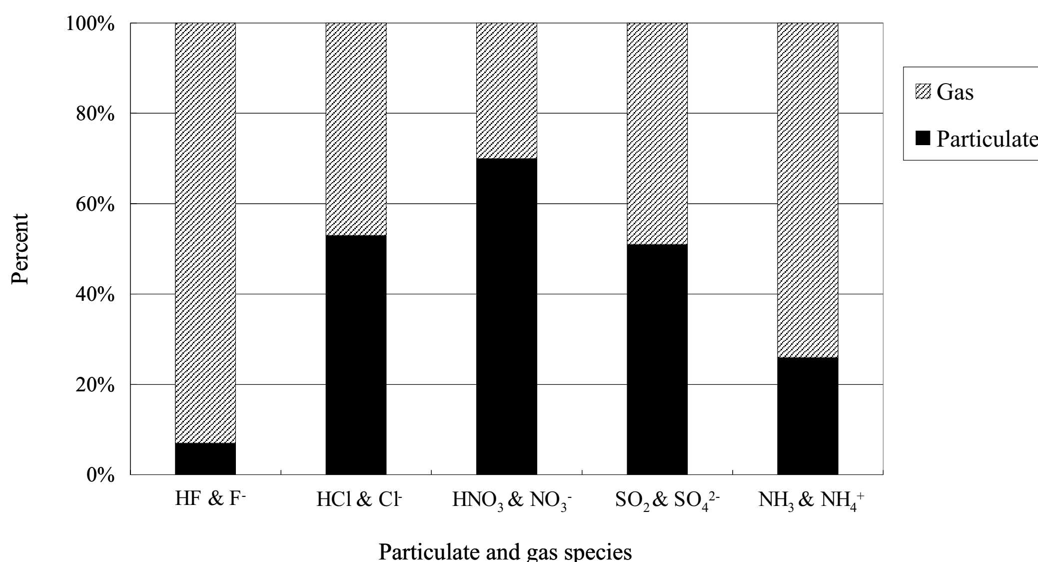

Fig. 4(b). Fractional distribution of each inorganic species in gas and particulate phases at etch area.

higher concentration than their particulate phase of F^- and NH_4^+. This was also observed previously in Fig. 2 that both of their gas phase concentrations could be higher than 5 ppbv. Thus it indicates their major sources were from local emissions of chemicals used in the fab process.

Based on the above discussion, a summary of possible inorganic AMCs sources detected at the photo and etch areas is given in Table 5. Most of airborne contaminants in the fab come from the process chemicals, outside air and process tools. However, depending on the airflow design, some areas can contaminate adjoining ones due to recirculation. The fab exhaust, even adequately scrubbed to meet regulatory requirements at parts per million (ppm) levels, can be pulled back into the fab on a calm day by the air intakes and cause contamination problems. Facilities building and clean room construction materials, people and internal activities can also be significant sources of contamination.

CONCLUSIONS

The results of actual clean room sampling showed that the major inorganic gas species in a cleanroom were NH_3 and HF. The average $PM_{2.5}$ mass concentrations were 17.52 and 18.23 μg/m^3 at the photo and etch areas, respectively. The inorganic species account for over 50% of $PM_{2.5}$ mass. The Na^+, NH_4^+, Cl^- and SO_4^{2-} concentrations in particulates dominated the identifiable components, and total occupied 46.4% and 46.9% of $PM_{2.5}$ mass at the photo and etch areas, respectively.

Considering the fact that the molar ratios of ammonium to sulfate ranged over 2, it is inferred that they formed sufficiently neutralized compounds such as $(NH_4)_2SO_4$ as the leading constituent in cleanroom environments. High correlations are noted between NH_4^+ and SO_4^{2-} at both the photo and etch sampling areas. It is known that when

Table 5. Summary of possible sources of gas and particulate species at the photo and etch areas.

Type	Species	Photo area		Etch area	
		Sources	Notes	Sources	Notes
Gas phase	HF	Outdoor contaminants	-	Outdoor contaminants	-
		-	-	Wet bench chemicals (HF, BOE and M1)	R^2: 0.70 (HF vs. NH_3)
		-	-	Reactive ion from the dry etchers	-
	HCl	Outdoor contaminants	-	Outdoor contaminants	-
		-	-	Wet bench chemicals (HCl and SC2)	-
		-	-	Reactive ion from the dry etchers	-
	HNO_2	Outdoor contaminants	-	Outdoor contaminants	-
	HNO_3	Outdoor contaminants	-	Outdoor contaminants	-
		-	-	Wet bench chemicals (M1 and M2)	-
	SO_2	Outdoor contaminants	-	Outdoor contaminants	-
		-	-	Reduction of wet bench chemicals (H_2SO_4)	-
		-	-	Reactive ion from the dry etchers	-
	NH_3	Outdoor contaminants	-	Outdoor contaminants	-
		Human exhaled breath	-	Human exhaled breath	-
		DUV Process chemicals (Amines, HMDS and TMAH)	-	Wet bench chemicals (NH_4OH, BOE and SC1)	-
Particle phase	Cl^-	Indoor gas to particle conversion/ outdoor contaminants	R^2: 0.49 (Cl^- vs. NH_4^+)	Indoor gas to particle conversion/ outdoor contaminants	R^2: 0.61 (Cl^- vs. NH_4^+)
	NO_3^-	HNO_3 condensed onto NH_4^+ containing particles	R^2: –0.73 (HNO_3 vs. NH_4^+)	-	-
		Outdoor contaminants	-	Outdoor contaminants	-
	SO_4^{2-}	Indoor gas to particle conversion/ outdoor contaminants	R^2: 0.62 (SO_4^{2-} vs. NH_4^+)	Indoor gas to particle conversion/ outdoor contaminants/etching acids (H_2SO_4)	R^2: 0.82 (SO_4^{2-} vs. NH_4^+)
	Na^+	Human emissions	-	Human emissions	-
		Positive photoresists process	-	Photoresists stripping by plasma process	-
	NH_4^+	Indoor gas to particle conversion/ outdoor contaminants	-	Indoor gas to particle conversion/ outdoor contaminants	-
		Human emissions	-	Human emissions	-
		NH_3 condensed onto NO_3^- containing particles	R^2: –0.68 (NH_3 vs. NO_3^-)	-	-
	K^+	Positive photoresists process	-	Photoresists stripping by plasma process	-
		-	-	KOH or water deep etching environment	-
	Ca^{2+}	Positive photoresists process	-	Photoresists stripping by plasma process	-

wafers are washed with a chemical based on sulfuric acid, their surface could be frosted by ammonium sulfate because of the abundance of ammonia in the clean room. It was observed that relatively high fraction of Cl^-, NO_3^- and SO_4^{2-} existed in particulate phase while F^- and NH_4^+ were mainly in gas phase as HF and NH_3 gaseous species.

REFERENCES

Adachi, M., Okuyama, K., Tohge, N., Shimada, M., Sato, J. and Muroyama, M. (1994). Precursors in an Atmospheric-Pressure Chemical Vapor Deposition of Silica Films from Tetraethylorthosilicate/Ozone System. *Jpn. J. Appl. Phys.* 33: L447–L450.

Bai, H., Kang, Y. and Liu C. (2002). Dimensional and Elemental Analysis of Particulate Contaminations on Silicon Wafers. *Aerosol Air Qual. Res.* 2: 53–60.

Chien, C.L., Tsai, C.J., Ku, K.W. and Li S.N. (2007). Ventilation Control of Air Pollutant during Preventive Maintenance of a Metal Etcher in Semiconductor Industry. *Aerosol Air Qual. Res.* 7: 469–488.

Constant, I., Tardif, F. and Derrien, J. (2000). Deposition and Removal of Sodium Contamination on Silicon Wafers. *Semicond. Sci. Technol.* 15: 61–66.

Friedlander, S.K. (2000). *Smoke, Dust, and Haze: Fundamentals of Aerosol Dynamics*, Oxford University Press, New York.

Fu, W.S., Chen, S.F. and Yang S.J. (2001). Numerical Simulation of Effects of Moving Operator on the Removal of Particles in Cleanroom. *Aerosol Air Qual. Res.* 1: 37–45.

Hinds, W.C. (1999). *Aerosol Technology：Properties,*

Behavior, and Measurement of Airborne Particles, 2nd edition, John Wiley & Sons, New York.

Huang, C.H., Ho, Y.T. and Tsai, C.J. (2005). Measurement of Inorganic Acidic Gases and Particles from the Stack of Semiconductor and Optoelectronic Industries. *Sep. Sci. Technol.* 39: 2223–2234.

Johnstone, E.V., Chovino. C., Reyes, J. and Dieu, L. (2004). Haze Control: Reticle/Environment Interactions at 193 nm. *Solid State Technol.* 47: 69–73.

Kinkead, D., Joffe, M., Higley, J. and Kishkovich, O. (1995). *Forecast of Airborne Molecular Contamination Limits for the 0.25 micron High Performance Logic Process*. in Technology Transfer #95 052 812A-TR SEMATECH.

Kitajima, H. and Shiramizu, Y. (1997). Requirements for Contamination Control in the Gigabit Era. *IEEE Trans. Semicond. Manuf.* 10: 267–272.

Li, S.N., Shih, H.Y., Yen, S.Y. and Yang, J. (2007). Case Study of Micro-Contamination Control. *Aerosol Air Qual. Res.* 7: 432–442.

Lin, I.K., Bai, H., Liu, C.C. and Wu, B.J. (2008). Comparison of Cleanroom Samplers for Inorganic Airborne Molecular Contaminants. *Sep. Sci. Technol.* 43: 842–861.

Lin, I.K., Bai, H. and Wu, B.J. (2009). Surface Deposition of Ionic Contaminants on Silicon Wafers in a Cleanroom Environment. *IEEE Trans. Semicond. Manuf.* 22: 321–327.

Lue, S.J. and Huang, C. (1999). Applications of Ion Chromatography in the Semiconductor Industry. II. Determination of Basic Airborne Contaminants in a Cleanroom. *J. Chromatogr. A.* 850: 283–287.

Lue, S.J., Wu, T., Hsu, H. and Huang, C. (1998). Application of Ion Chromatography to the Semiconductor Industry. I. Measurement of Acidic Airborne Contaminants in Cleanrooms. *J. Chromatogr. A*. 804: 273–278.

MacDonald, S.A., Hinsberg, W.D., Wendt, H.R., Clecak, N.J. and Willson, C.G. (1993). Airborne Contamination of a Chemically Amplified Resist. 1. Identification of Problem. *Chem. Mater.* 5: 348–356.

Pio, C.A. and Harrison R.M. (1987). Vapour Pressure of Ammonium Chloride Aerosol: Effect of Temperature and Humidity. *Atmos. Environ.* 21: 2711–2715.

Poling, B.E., Prausnitz, J.M. and O'Connell, J.P. (2001). *The Properties of Gases & Liquids*, McGraw-Hill, New York.

Saiki, A., Oshio, R., Suzuki, M., Tanaka, A., Itoga, T. and Yamanaka, R. (1995). Development of Ammonia Adsorption Filter and its Application to LSI Manufacturing Environment. *J. Photopolym. Sci. Technol*. 8: 599–606.

Seinfeld, J.H. and Pandis, S.N. (2006). *Atmospheric Chemistry and Physics: From Air Pollution to Climate Change,* 2nd edition, John Wiley & Sons, New York.

Stelson A.W. and Seinfeld, J.H. (1982). Relative Humidity and Temperature Dependence of the Ammonium Nitrate Dissociation Constant. *Atmos. Environ.* 16: 983–992.

Tsai, C.J., Huang, C.H., Lin, Y.C. and Shih, T.S. (2003). Field Test of a Porous-metal Denuder Sampler. *Aerosol Sci. Technol.* 37: 967–974.

Warneck, P. (2000). *Chemistry of the Natural Atmosphere* 2nd edition, International Geophysics, Academic Press, New York.

Ye, Y., Liu, B.Y.H. and Pui, D.Y.H. (1993). Condensation-induced Particle Formation during Vacuum Pump Down. *J. Electrochem. Soc*. 140: 1463–1468.

Yeh, C.F., Hsiao, C.W., Lin, S.J., Hsieh, C.M., Kusumi, T., Aomi, H., Kaneko, H., Dai, B.T. and Tsai, M.S. (2004). The Removal of Airborne Molecular Contamination in Cleanroom Using PTFE and Chemical Filters. *IEEE Trans. Semicond. Manuf.* 17: 214–220.

Zhuang, H., Chan, C.K., Fang, M. and Wexler, A.S. (1999). Size Distributions of Particulate Sulfate, Nitrate, and Ammonium at a Coastal Site in Hong Kong. *Atmos. Environ*. 33:843–853.

Received for review, October 15, 2009
Accepted, January 12, 2010